

ICANS XIV
14th Meeting of the International Collaboration on
Advanced Neutron Sources
June 14-19, 1998
Starved Rock Lodge, Utica, IL

HELIOS: A High Intensity Chopper Spectrometer at LANSCE

T.E. Mason^{1,2}, C. Broholm³, B. Fult⁴, R. Osborn⁵, R.A. Robinson⁶, G. Aeppli⁷,
H.A. Mook¹, S.E. Nagler¹, B. Keimer⁸ and S. Kern⁹

¹Oak Ridge National Laboratory, Oak Ridge TN 37831

²Department of Physics, University of Toronto, Toronto, ON M5S 1A7, Canada

³Department of Physics and Astronomy, The Johns Hopkins University,
Baltimore MD 21218

⁴Department of Materials Science, California Institute of Technology,
Pasadena CA 91125

⁵Argonne National Laboratory, Argonne IL 60439

⁶Los Alamos National Laboratory, Los Alamos NM 87545

⁷NEC Research Institute, 4 Independence Way, Princeton NJ 08540

⁸Department of Physics, Princeton University, Princeton NJ 08544

⁹Department of Physics, Colorado State University, Fort Collins CO 80523

Abstract

A proposal to construct a high intensity chopper spectrometer at LANSCE as part of the SPSS upgrade project is discussed. HELIOS will be optimized for science requiring high sensitivity neutron spectroscopy. This includes studies of phonon density of states in small polycrystalline samples, magnetic excitations in quantum magnets and highly correlated electron systems, as well as parametric studies (as a function of pressure, temperature, or magnetic field) of $S(\mathbf{Q},\omega)$. By employing a compact design together with the use of supermirror guide in the incident flight path the neutron flux at HELIOS will be significantly higher than any other comparable instrument now operating.

Introduction

We propose the construction of a high intensity, direct-geometry, time-of-flight spectrometer, HELIOS, on flight path 8 at the Lujan Center. HELIOS will be optimized to provide the highest possible neutron flux at the sample, high detection efficiency, and sufficient energy resolution to study dynamical processes in a wide variety of materials. The spectrometer will be capable of using the full energy spectrum of neutrons provided by a water moderator at a spallation neutron source, making it useful for studies of excitations from a few meV to several hundred meV. The performance at the lower end of this range will be boosted by supermirrors in the incident flight path. HELIOS will be compact, with a source-sample distance of 7.1 m and a secondary flight path of 2.5 m. The short secondary flight path will allow for a dense array of position-sensitive detectors that will be able to detect the direction and velocity of almost 10% of the neutrons scattered by the sample. Design calculations show that HELIOS would be the most efficient chopper spectrometer at any spallation neutron source.

The scientific mission for HELIOS is to enhance our fundamental understanding of materials by providing detailed information about their dynamic processes. Research topics include: (i) studies of vibrational excitations and their relationship to phase diagrams and equations of state of materials, including materials with correlated electrons, and (ii) studies of spin correlations in magnets, superconductors, and materials close to metal-insulator transitions. The projects described in the proposal are at the forefront of current civilian research in condensed matter physics and materials science, but some are relevant to the SBSS program. For example studies of the phase diagram of cerium and electronic correlations in f-electron metals are closely linked to understanding the complicated phase diagram of plutonium. In addition HELIOS would be the instrument of choice for studies of phonons and the magnetic susceptibility of plutonium metal under pressure or over a range of temperatures.

Optimized for efficiency, the HELIOS spectrometer would enable civilian and weapons programs to acquire data over a range of physical parameters, such as mapping dynamic processes in solids as a function of temperature, pressure and composition. Such parametric studies on HELIOS will provide physical trends in microscopic dynamical properties over energies from 1-500 meV. Mapping such physical trends is largely impractical with today's instrumentation at LANSCE or elsewhere.

The design of a new chopper spectrometer and its integration into the Lujan Center facilities will require an extensive effort on instrument design. Much of this work will be done under the auspices of the instrumentation R&D program of the Spallation Neutron Source, a collaboration between Oak Ridge and Argonne. Funding for the design effort will be obtained largely from the SNS allowing an immediate start, independent of Los Alamos funding commitments. It is expected that the design will be ready once construction funds are available in late 1999.

The HELIOS spectrometer is a natural complement to the higher resolution PHAROS instrument at LANSCE. Having both instruments at the same laboratory will allow the design of experiments where initial surveys and parametric studies are conducted on HELIOS, while details of energy spectra under selected conditions are measured by PHAROS. The addition of the HELIOS spectrometer will provide the Lujan Center a unique opportunity to become an international center for experimental research at the forefront of condensed matter physics and materials science.

1 Scientific Justification

Neutron spectroscopy provides unique information about dynamic properties of condensed matter. Time and again this experimental technique has yielded critical information towards the understanding of the fundamental properties of condensed matter. Neutron spectroscopy provided comprehensive evidence for phonons and the first evidence for spin waves by directly probing the corresponding dispersion relations. Brockhouse was awarded the 1994 Nobel Prize in physics for such work.

A neutron spectrometer provides optimal sensitivity and resolution only in a limited range of energy and wave vector transfer. So, while there are a number of highly productive neutron scattering spectrometers currently operating in the United States, no instrument offers state-of-the-art sensitivity towards wave vector resolved magnetic and vibrational dynamics in the energy range from 50 to 500 meV. None have the efficiency of the proposed HELIOS instrument, which will enable rapid data acquisition over a wide range of experimental parameter space. In this section we discuss the scientific areas which are currently suffering from this lack of suitable instrumentation and which would greatly benefit from an instrument such as HELIOS.

1.1 Lattice Dynamics

The past two decades have seen a steady growth in our understanding of alloy phase diagrams. There has been excellent progress in the ab-initio microscopic approach, which provides a free energy function by combining total electronic energy calculations with an entropy from statistical mechanics¹. Almost every experimental discovery of an important new alloy such as a high temperature superconductor or a high strength transition metal aluminide is now followed quickly by a phase diagram calculation. While these phase diagrams are not necessarily precise in detail, they are helpful for further materials development. B. Fultz and his group would use the HELIOS spectrometer for investigations in the field of alloy phase stability, specifically on the vibrational entropy of alloy phases. The free energy, F , of an alloy phase is:

$$F = E - T(S_{\text{config}} + S_{\text{vibr}}) \quad (1)$$

The configurational entropy, S_{config} , is well known, and methods for calculating S_{config} are well developed. Until recently, however, S_{vibr} , has been essentially unknown and assumed to be small.

Precision calorimetry measurements^{2,3,4,5} have shown that for chemically ordered and disordered Ni_3Al , Fe_3Al , Cu_3Au , and Co_3V , the difference in vibrational entropy between alloy phases is typically $0.2 k_B/\text{atom}$. This is about half the size of the difference in configurational entropy during a phase transition, and vibrational entropy will therefore make a major contribution to the alloy free energy. The difference in vibrational entropy originates with the phonon density of states (DOS, $g(E)$) of the alloy. In the high temperature limit the difference in

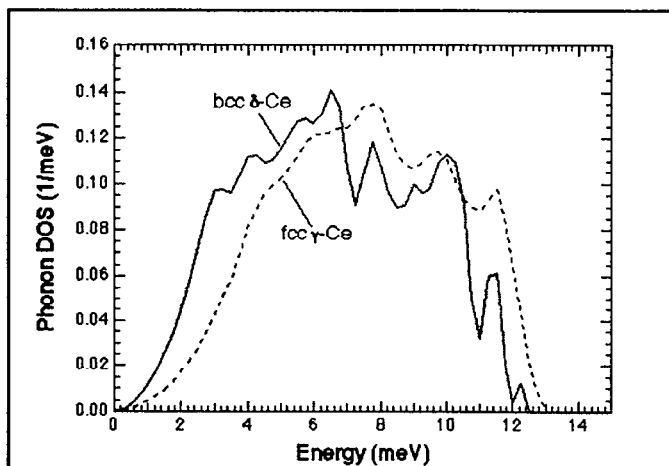


Figure 1: Phonon DOS curves of fcc cerium at 984 K and bcc cerium at 1028 K. Spectra were acquired at 5 values of Q , chosen by prior calculation of the polycrystalline average of the coherent scattering from the fcc phase. Spectra were corrected individually for multi-phonon scattering and background, and summed.

vibrational entropy between two phases, α and β , is:

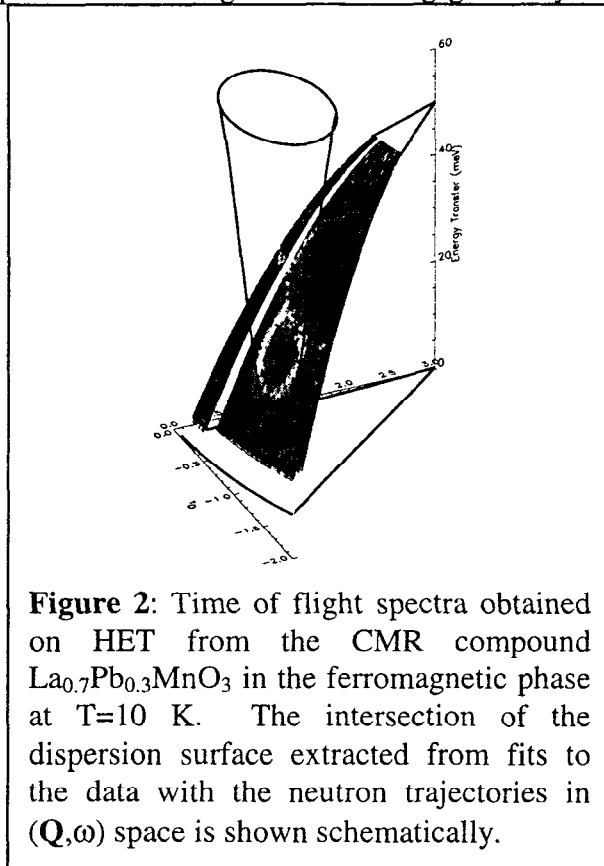
$$\Delta S_{vibr}^{\alpha-\beta} = 3k_B \int_0^{\infty} [g^{\beta}(E) - g^{\alpha}(E)] \ln(E) dE \quad (2)$$

where the difference of normalized DOS functions avoids problems with the dimensionality of the logarithm. B. Fultz's group is now actively measuring differences in the phonon DOS curves of different alloy phases. The disordered states of most materials of interest cannot be obtained in single crystals, so polycrystalline materials must be used for the neutron scattering measurements. Measurements on Fe_3Al , Ni_3Al , Ni_3V , and Co_3V , gave DOS curves in good agreement with calorimetry results^{2,3,5,6,7} (using the finite temperature equivalent of Eq. (2)). We are also investigating how microstructural features affect the vibrational entropies of materials^{8,9}. In collaboration with R. A. Robinson (LANL), G. H. Kwei (LANL), R. J. McQueeney (LANL), and J. L. Robertson (ORNL), B. Fultz's group recently made inelastic neutron scattering measurements at HFIR, ORNL on the fcc - bcc phase transition in cerium metal. Tentative DOS curves are presented in Figure 1.

Notice that the phonon DOS of the bcc phase is shifted significantly to lower energies with respect to the fcc curve, suggesting a softening of one or more of the transverse branches. Most significantly, the observed change in phonon DOS predicts a change in vibrational entropy of 0.6 k_B /atom, using Eq. (2). This is actually larger than expected from the latent heat of the fcc - bcc transition, and suggests that there may be a change in the electronic entropy of cerium during the fcc - bcc transition. Our experiments to measure phonon DOS curves of different alloy phases almost invariably require the use of polycrystalline samples, for which a direct-geometry time-of-flight spectrometer offers advantages such as the absence of contamination wavelengths and simultaneous data collection over a wide range in Q . The energy resolution need not be particularly high, since we are interested primarily in comparative studies between different states of a material. For the purpose of obtaining thermodynamic information, high energy resolution is not required anyhow, since Eq. (2) is an average over the phonon DOS. In general we do not need to identify specific features of phonon DOS curves. In cases where this need arises, however, the PHAROS II spectrometer will be a well-matched companion. The HELIOS spectrometer would be ideal for much of our present work, and will provide new research opportunities. For example, it is now impractical for us to obtain more than two or three phonon DOS curves in an experimental session. With HELIOS, however, we expect to be able to follow the evolution of the phonon DOS at intermediate states of a phase transition. The evolution of vibrational entropy may play a central role in the kinetics of some phase transitions, but this is as yet an unexplored topic in materials science.

1.2 Magnetic Dynamics

Direct-geometry time-of-flight spectrometers offer a powerful probe for studying the magnetic dynamics in materials, offering a wide range of frequencies together with the ability to map out a large region of reciprocal space. Many of the most celebrated successes in applying the direct-geometry time-of-flight method to studies of magnetic dynamics have been in the study of low-dimensional materials. In such systems it is possible to arrange the scattering geometry so the simultaneous variation of momentum



and energy transfer along a time of flight trajectory is projected out - giving full coverage of the 1D or 2D reciprocal space. This is not essential however, a recent example is the measurements obtained on HET showing a cut through the very three dimensional dispersion surface of a manganese oxide, one of the so called Colossal Magneto-Resistive (CMR) compounds¹⁰, shown in [Figure 2](#).

Note that the range of energy transfers accessed in this measurement (0-50 meV) is much lower than that generally thought to be optimal for this class of instrument. The provision of incident flight path supermirror guides on HELIOS will further improve its efficiency below about 25 meV.

An example of the use of a direct-geometry time-of-flight spectrometer for the studies of the magnetic dynamics in

a low-dimensional material is a measurement of the spin wave in FeGe_2 (a quasi-one-dimensional itinerant antiferromagnet) performed on HET, mapping out the c-axis dispersion up to 400 meV. [Figure 3](#) shows data obtained in ~6 hours using an incident energy of 120 meV at 11 K. In low-dimensional compounds it is possible to characterize a large fraction of the dispersion surface in a single geometry since the variation of \mathbf{Q} along a weakly coupled direction in the (\mathbf{Q},ω) trajectories does not affect the excitation energy. In the case of FeGe_2 the Q_a variation is negligible so the (Q_c,ω) dispersion is mapped out from 40 - 100 meV¹¹.

G. Aeppli, C. Broholm, B. Keimer, T. E. Mason, H. A. Mook, R. Osborn, and R. A. Robinson share an interest in the structure and spin dynamics in correlated electronic materials. The quest for a theoretical description of materials with strong electron-electron interactions is currently at the forefront of condensed matter physics, and the correlation functions measurable by inelastic magnetic neutron scattering provide unique and incisive constraints for theories of the

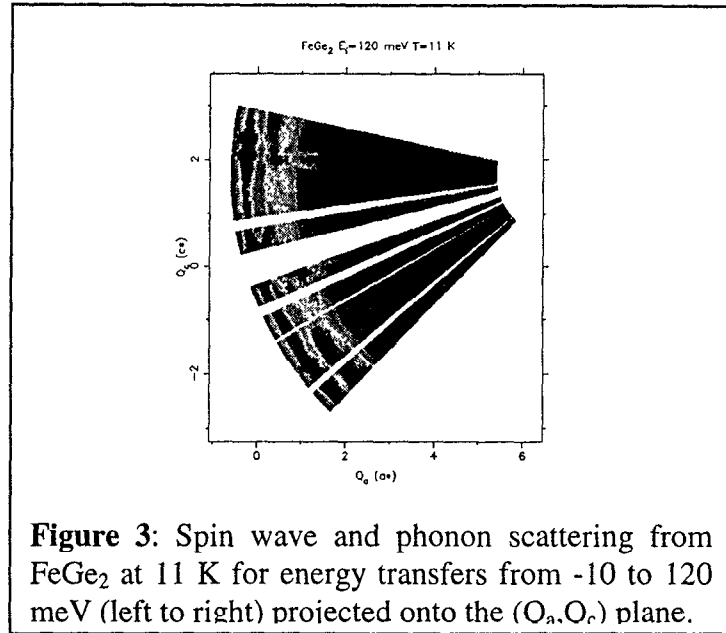


Figure 3: Spin wave and phonon scattering from FeGe₂ at 11 K for energy transfers from -10 to 120 meV (left to right) projected onto the (Q_a, Q_c) plane.

electronic many-body states realized in these materials. Unfortunately there is, however, no instrument in the US that can efficiently probe electronic correlations at energies beyond 50 meV. This has limited the application of neutron spectroscopy to a relatively small class of materials with low temperature anomalies of little technological significance. By increasing the range of energies and reducing the required sample size, HELIOS would expand the range of materials that can be studied by neutron spectroscopy. With HELIOS we could study spin dynamics in correlated metals with energy scales from 10-500 meV. There is no reason to expect the microscopic information about electronic correlations in these materials to be less interesting than what we learned from neutron spectroscopy in heavy fermion systems where the energy scales are an order of magnitude smaller. High T_c superconductors are important examples of interesting correlated metals but we may also make progress in understanding seemingly less exotic 3d metals such as chromium, yttrium, vanadium, or even copper, where the energy scale for magnetic excitations is set by the Fermi energy. Experiments in magnetic multilayers have shown that these materials have considerable Q -dependence in their magnetic susceptibility. New microscopic information about electronic correlations in these systems could have an important impact on our understanding of electronic correlations in the metallic state.

1.2.1 High Temperature Superconductivity

The supreme challenge in the field of strongly correlated electron systems is an explanation of high temperature superconductivity in the quasi-two dimensional cuprates. A central question in the theory of high temperature superconductors is the relationship between the microscopic spin dynamics and the transport and superconducting properties of the cuprates. To this end, knowledge of the spin correlations over a wide energy range is essential. Until recently, such experiments were confined to excitation energies below ~ 40 meV, larger than the superconducting energy gap but smaller than the intralayer superexchange $J \sim 120$ meV which sets the energy scale for spin excitations in the

undoped antiferromagnetic precursor compounds. In recent pioneering studies, many of the members of this SDT have extended these measurements to higher energies and established the presence of significant spectral weight at energies comparable to J in the $\text{La}_{2-x}\text{Sr}_x\text{CuO}_4$ and $\text{YBa}_2\text{Cu}_3\text{O}_{6+x}$ families of superconducting cuprates^{12,13,14}. The capability of carrying out such high-energy studies with sufficient intensity is currently lacking in the United States, and all of these important experiments were carried out at ISIS or European reactor sources with hot moderators. The HELIOS spectrometer would thus fill a critical need in this regard. Regular access to a high-intensity spectrometer would enable us to obtain detailed, quantitative measurements of the temperature and doping dependence of the high energy spin dynamics in the cuprate high- T_c materials which are essential for microscopic theories of high temperature superconductivity.

Crystal field spectroscopy is another promising tool to study the electronic state of the cuprate superconductors. S. Kern's research has been primarily focused on studying the excitations in polycrystalline samples, both electronic and lattice. A high-intensity spectrometer is useful for detecting the often weak response from magnetic systems. The ability to investigate electronic transitions and quasielastic scattering both at large and small incident energies makes a machine such as HELIOS very useful. For example, Kern has used an incident energy of 4 meV on HRMECS to determine the presence of ~ 1 meV crystal-field level in an Erbium high T_c material¹⁵. The line width of crystal field excitations has been shown to contain important information about the electronic susceptibility and the pairing state in the cuprates¹⁶. R. Osborn and collaborators have reported transitions in f -electron systems reaching to the 1 eV range¹⁷. In S. Kern's recent investigations of the interactions between the electrons and phonons in the rare-earth phosphates, both small scattering angle coverage (low Q) for the electronic transitions and wide angle coverage for the phonons (high Q) were needed. Low noise in the forward scattering direction is required for accurate determination of magnetic response.

A quantitative understanding of high temperature superconductivity in the cuprates will ultimately require broad, systematic studies of transition metal oxides as a function of parameters such as the carrier concentration, dimensionality, the width of the valence band, correlation and charge transfer energies, and disorder. Many of the members of this SDT collaborate actively with solid state chemists and materials scientists at their institutions and elsewhere who are capable of growing high quality single crystals of a wide variety of these materials.

1.2.2 One Dimensional Quantum Magnets

Undoped spin chain compounds are arguably the simplest realizations of quantum many body systems and have for years served as a unique "laboratory" for many-body physics. Some idealized spin chain Hamiltonians can actually be solved exactly; their excitation spectra consist of sharp, dispersive modes and excitation continua. While the spin-wave-like dispersive modes have been studied by neutron scattering since the 1970's, the quantitative exploration of excitation continua has been greatly advanced by direct-geometry time-of-flight spectrometers at pulsed neutron sources. A high flux chopper spectrometer like HELIOS would be the ideal instrument for investigating such broad, diffuse inelastic scattering, and would have a large impact on research in this area. For

example, S. E. Nagler's work employed MARI to study the free spinon continuum spectrum in the $S=1/2$ Heisenberg antiferromagnetic chain system KCuF_3 ¹⁸. Direct measurements of the dynamic spin correlation function, $S^{\text{aa}}(\mathbf{Q},\omega)$, were made possible by orienting the sample with the chain axis parallel to the incident neutron direction, resulting in magnetic scattering with azimuthal symmetry. This allowed integration of the signal over many detectors without loss of information. A complementary approach (see for example, work on CuGeO_3 by M. Arai and co-workers) attempts to survey large regions of reciprocal space simultaneously. This method was used to measure a similar continuum in the spin-Peierls compound CuGeO_3 ¹⁹. These experiments have tested many aspects of one-dimensional quantum magnetism for the first time, and have also revealed unanticipated features such as a "double gap" structure in alternating spin chains^{20,21}. Other members of this collaboration have focused on the effect of high magnetic fields on organic and inorganic spin chain compounds and discovered novel field-induced fluctuations²² and phase transitions²³. The theoretical description of these phenomena is still in its infancy. HELIOS will open up many new experimental opportunities along these lines, such as the study of new spin chain compounds with different alternation parameters, higher-lying excitations continua etc.

The gap from one to two dimensions can be bridged by spin-ladders, realized in compounds with two or more directly adjacent, strongly interacting spin chains²⁴. Several cuprate spin ladders have been identified, including one that can be doped and becomes superconducting under pressure²⁵. Since many of these materials are characterized by exchange constants comparable to or larger than the high- T_c compounds²⁶, HELIOS would again be well suited to study their spin dynamics. Efforts to synthesize large crystals of cuprate and cobaltate spin ladders are underway in the laboratory of R. Cava at Princeton University, a collaborator of B. Keimer, using a new floating zone furnace. S. E. Nagler's group is studying chain/ladder systems in the vanadium phosphate family²⁰.

1.2.3 Metal Insulator Transition in Oxides

Oxides of 3d metals other than copper also show intriguing behavior dominated by electronic correlations. R. Osborn has started a program to study the magnetic correlations close to the metal-insulator transition in $\text{La}_{1-x}\text{Sr}_x\text{TiO}_3$, a three-dimensional electron analogue to the well known hole-doped cuprate $\text{La}_{2-x}\text{Sr}_x\text{CuO}_4$. These compounds undergo a Mott-Hubbard transition at $x \sim 0.05$, which is accompanied by a divergence of the d-electron effective mass according to specific heat and magnetic susceptibility²⁷. This is predicted to produce a narrowing of the energy scale of d-electron magnetic fluctuations into the range accessible by HELIOS. Early studies indicate that the response is enhanced close to the transition, but is difficult to determine unambiguously because of the limited sensitivity of current instrumentation. Optimized for sensitivity in the relevant energy range, HELIOS will enable single crystal investigations of the transition to the Mott-insulating antiferromagnetic phase. G. Aeppli and collaborators are studying manganites of composition $\text{La}_{1-x}\text{Pb}_x\text{MnO}_3$ which are fully spin polarized metals by virtue of the double-exchange mechanism. The same microscopic physics also underlies the recently discovered "colossal magnetoresistance" effect that has potential for technological applications. While these materials have been known for more than 40 years, an experimental characterization of the excitations of the

double-exchange Hamiltonian has only recently been achieved through studies at ISIS¹⁰. The manganites show rich phase diagrams with competing charge-localized and metallic states whose spin dynamics is only beginning to be probed. The flexibility and dynamic range of HELIOS will undoubtedly prove useful in this area as well.

Whereas various 3d metal oxides are currently under intense investigation in laboratories around the world, compounds based on 4d/5d transition metals are potentially very interesting materials that are only now beginning to attract serious attention of condensed matter physicists. The large size of the outer electron cloud in the 4d/5d series results in greatly increased hybridization and potentially new physics. For this reason we call such materials "extended electron" compounds. Examples of recent interest include SrRuO₃, which is a "badly metallic" ferromagnet (i.e. with electronic properties similar to those of the normal state of high T_c superconductors, fullerenes, and organic metals), and the derivative compound Sr₂RuO₄, now suspected to be a p-wave superconductor²⁸. There is much to be learned by studying the magnetic fluctuation spectrum of such materials, and in some cases perhaps even optical phonons. There are several technically challenging aspects of such measurements that may be well suited to HELIOS. The rapidly diminishing form factors force measurements with high energy transfers at small wavevectors. Typically only small single crystals or powders are available. The itinerant nature of the magnetism in many of these materials also can result in excitation continua. The effective dimensionality of the ruthenates, as well as that of the cuprates, can be systematically changed in the Ruddlesden-Popper scheme which interpolates quasi-continuously between two and three dimensional electronic structure by changing the number of directly adjacent transition metal oxide layers, resulting in compounds such as Sr₂RuO₄, Sr₃Ru₂O₇, etc. Ruthenates of this series will be studied by S. E. Nagler, while B. Keimer plans experiments on analogous cuprate compounds to be synthesized in R. Cava's laboratory.

1.2.4 Heavy Fermion Magnetism

There are also exciting developments in the area of heavy fermion systems to which experiments at HELIOS could make important contributions. R. Osborn will use HELIOS in studies of the dynamic susceptibility of disordered heavy fermions, usually containing uranium ions that exhibit unusual power-law correlations at low temperature. Pulsed neutron spectroscopy at IPNS and ISIS have already revealed a novel scaling of the magnetic response which is universal in ω/T over a very wide dynamic range of frequencies and temperatures²⁹. This is believed to result from quantum critical scattering associated with the proximity to a T=0 phase transition. A key question to be resolved is the dimensionality of the correlations. At high temperatures (>30K), the scattering is single-ion in nature but there is evidence of a crossover at low temperatures to a quantum-disordered regime showing weak antiferromagnetic correlations. The scaling properties are reminiscent of marginal Fermi liquids, proposed to explain the unusual normal-state properties of high-temperature superconductors, which also undergo quantum phase transitions as a function of doping. We intend to pursue the systematics of this scaling as a function of composition and other thermodynamic variables. Pulsed neutron time-of-flight spectrometers have been especially valuable in determining this

scaling behavior because of the wide range of accessible energies and angles. The angular range is also necessary in subtracting the phonon scattering reliably³⁰.

1.2.5 Characterization of Novel Magnetic Materials

The vast majority of novel magnetic materials are developed by solid state chemists through guided trial and error using susceptibility and perhaps specific heat measurements as the diagnostic tools. Because current neutron scattering instrumentation requires large amounts of material this powerful sample characterization tool is typically only applied by specialists as a means of explaining previously discovered anomalies. Optimized for high sensitivity HELIOS will enable rapid surveys of spin fluctuations in new materials that are available only in small quantities. We expect that this will make neutron spectroscopy an important tool for the initial characterization of novel magnetic materials thus bringing more detailed information about a larger amount of different materials to a broader community of materials scientists.

1.3 Relevance of HELIOS to the Weapons Program

1.3.1 Introduction

While we are primarily interested in f-electron systems because of their fascinating correlated-electron properties, as manifest in heavy fermion, non-Fermi-liquid, superconducting and other behaviors, the same issues are important in understanding the basic properties of nuclear-weapons materials, in particular plutonium. It has long been known that, part way across the actinide row of the Periodic Table, there is a transition from itinerant electronic behavior (as typically occurs in the transition metals) to more localized f-electron behavior (as in the rare earths). Plutonium lies right at the crossover between the two regimes^{31,32}. This means that first-principles one-electron band-structure calculations of plutonium are not reliable, and there is a need for experimental data (on phonons and the enhanced generalized magnetic susceptibility) on the various different phases of plutonium. Given such data, it should be possible to learn how to include correlations within the electronic-structure calculations. Accurate electronic structure calculations of actinides are an important part of the Science Based Stockpile Stewardship Program. We envisage a strong interplay between work on plutonium and civilian basic research on f-electron systems more generally, because the underlying physics is so closely related.

The PHAROS spectrometer at LANSCE is beginning to make important contributions to the LANL effort in Science Based Stockpile Stewardship. In the next LANSCE operating cycle, it is expected that a number of important measurements on ²⁴²Pu will be performed with PHAROS. The excellent energy resolution of the PHAROS spectrometer makes it an ideal instrument for measuring the phonon densities of states and neutron Brillouin scattering from ²⁴²Pu at ambient temperature and pressure. It is also expected that PHAROS will be an excellent instrument for measuring dispersion curves from δ -²⁴²Pu once a single crystal is available. As described here, however, there are a number of important experiments for which the HELIOS spectrometer would be much more suitable than PHAROS, and HELIOS should enable new experimental investigations.

Most importantly, the HELIOS spectrometer will make possible experiments on Pu under pressure. The difficulty with neutron inelastic scattering experiments with samples under pressure is the scattering from the pressure cell. Scattering from the pressure cell can readily overwhelm the scattering from a small sample of a specialty isotope. The HELIOS design, with its high-intensity and oscillating radial collimators, will be ideal for measurements on small samples in a pressure cell. If HELIOS construction starts within a year, the pressure experiments on HELIOS should match well the timetable for the completion of a number of important experiments on ^{242}Pu with the PHAROS spectrometer. Although such work is classified, we present here some ideas for experiments on HELIOS, and we suggest these experiments are relevant to the SBSS mission.

1.3.2 Work on Ce Metal and its Relationship to Pu

Over the past year there has developed a collaboration between B. Fultz at Caltech and R. A. Robinson and G. H. Kwei at Los Alamos. Together with a bright LANL postdoctoral fellow, R. J. McQueeney, this group has already undertaken several productive collaborations on studies of phonons in metals using inelastic neutron scattering. We hope this ongoing interaction between university and LANL personnel will move forward into experiments of high relevance to the SBSS effort.

Quite independently, G. H. Kwei and B. Fultz recognized that the difficulty of performing experiments on plutonium would require practice with an analog material. Both concluded that cerium metal is the obvious choice. Cerium assumes four crystal structures at atmospheric pressure, and some transformations between these phases are related to electronic instabilities of its valence electrons. In this respect, cerium has similarities to plutonium metal, but is much easier to study. Experimental techniques for making measurements at different temperatures and pressures are now being refined through work on cerium metal, and these methods should later be applicable to studies on plutonium metal.

The first experiment resulted in a manuscript submitted to *Phys. Rev. Lett.*³³. It reports inelastic neutron scattering measurements on Ce metal at temperatures near the fcc (γ) to bcc (δ) transition, and presents approximate phonon DOS curves. A large difference in the phonon DOS of the γ -Ce and δ -Ce was found, providing a change in vibrational entropy at the γ - δ transition temperature of $(0.51 \pm 0.05) k_B \text{ atom}^{-1}$. To be consistent with the latent heat of the γ - δ transition, this large change in vibrational entropy must be accompanied by a thermodynamically significant change in electronic entropy of the opposite sign. This is the first evidence for a large electronic entropy contribution to the γ - δ phase transition. It is an exciting result, since it is the first case of a high-temperature structural phase transition in a material where electronic entropy is important. We expect that electronic entropy will play a similar role in the stability of the different solid phases of Pu metal.

Two more experiments on Ce were performed with the LRMECS spectrometer at IPNS at the Argonne National Lab. Data analysis for these measurements on Ce at low and high temperatures is still underway. It is expected that the anharmonicity of the phonons in fcc

γ -Ce will be determined. The heat capacity of γ -Ce has been measured at elevated temperatures, and it is considerably higher than the classical limit for a harmonic solid. Some of this excess heat capacity can be associated with the softening of the phonon DOS, but we also expect a contribution from the temperature-dependence of the electronic entropy in γ -Ce. Without electronic entropy, it can be shown that:

$$9 Bv \alpha^2 T = C_p(T) - C_v(T) = - \frac{T \Delta S_{vib}}{\Delta T}, \quad (3)$$

where ΔS_{vib} is defined as the change in vibrational entropy caused by the change in phonon DOS over the temperature range ΔT . While the first equality is rigorous (we derive this equality to impress students of thermodynamics with the power of the Maxwell relations), the second equality is true only if the electronic entropy is negligible. We are testing this relationship with the temperature dependence of the phonon DOS of γ -Ce. The same sort of experiments on δ - and δ' -Pu should be even more interesting, since their negative thermal expansion indicates that their anharmonicity is even larger. A temperature-dependence of the electronic entropy is a possible reason why phases in plutonium metal undergo negative thermal expansion.

In a preliminary experiment during our last beamtime allocation at LRMECS, we measured the phonon DOS of the shape memory alloy Ni-Ti³⁴. Data analysis is nearly complete, and some results are clear. There is a substantial difference between the phonon DOS of the high temperature "austenite" and low temperature "martensite" phases of NiTi. This difference is approximately consistent with the latent heat of the transformation measured by calorimetry. More specifically, it appears that most of this difference in vibrational entropy is caused by changes in low energy phonons. It is interesting that low energy phonons have also been associated with the displacive mechanism of the phase transformation in Ni-Ti³⁵.

1.3.3 Issues with Pu Metal

The phonon DOS of anharmonic solids will usually stiffen under pressure, leading to reduced entropy, for example. Another important consequence is an increase in the velocities of sound. At high pressures the increased speed of sound makes it possible to generate a shock wavefront that propagates through the material. Measuring the pressure dependence of phonon dispersion curves of a metal is an excellent way to understand the pressure conditions required for shock wave generation.

An unusual phenomenon should occur when driving high-pressure waves through a material with negative coefficient of thermal expansion such as δ -Pu. Negative thermal expansion indicates a negative Grüneisen constant, meaning that the phonon DOS of δ -Pu softens with increasing pressure. This would tend to suppress shock wave formation. However, it is not obvious that all phonon modes will have negative mode Grüneisen constants. For example, the phonon softening in Co_3V at elevated temperature is predicted very poorly with an average Grüneisen constant³⁶.

Studies on single crystals under pressure would provide the most useful data. Nevertheless, it should be possible to obtain some of this information with a mix of neutron Brillouin scattering and phonon DOS measurements. With the configuration of the PHAROS I spectrometer, B. Fultz, R. A. Robinson, and G. H. Kwei will soon attempt to measure an average dispersion of longitudinal waves from polycrystalline Ce metal. These neutron Brillouin scattering experiments can provide crystallographically averaged cuts through the dispersion surface of long wavelength phonons. Changes with temperature of the average intensities in the constant-energy cuts from these data, for example, should reveal the temperature-dependence of the average speed of longitudinal sound waves. The shapes of these measured intensity dispersions should provide the distribution of sound velocities along different crystallographic directions.

Beam collimation to suppress scattering from a pressure cell is difficult in forward geometry, however, so experiments with the sample under pressure cannot be performed so readily. Although these measurements will be attempted on PHAROS, it is likely that Brillouin scattering experiments will not be possible with the sample under pressure. It is most practical to characterize thoroughly the phonon DOS of Ce and ^{242}Pu with the PHAROS spectrometer with the sample at various temperatures. Pressure-dependent experiments are less appropriate for PHAROS.

The HELIOS spectrometer would be the ideal instrument for experiments on metals under pressure, owing to its higher intensity and its oscillating radial collimators. It is expected that by the time the HELIOS spectrometer is completed, the features of the phonon DOS of Ce and ^{242}Pu will be adequately understood so that it will be known which features of the phonon DOS correspond to which phonon polarizations.

Plutonium metal should exhibit a rich set of phase transitions at relatively modest pressures. We do not have access to classified literature on this subject, so the following comments must be considered speculative. Thermodynamically, however, the large specific volume of fcc $\delta\text{-Pu}$ must make it quite unstable against pressure-driven transformations (to $\alpha\text{-Pu}$, perhaps), and these should occur at pressures of several kbar. If the latent heat of these transformations have been measured under pressure, we should be able to determine independently the pressure dependencies of the electronic and phonon entropies. Furthermore, phonon softening may be a precursor to some of the low-temperature transformations in plutonium metal, which likely occur by diffusionless processes. Interpretations of the thermodynamics and kinetics of these transformations would proceed along the lines we are following for the work on NiTi^{34} .

1.3.4 Complementarity of HELIOS and PHAROS

The PHAROS weapons research effort will benefit from the development of HELIOS. An important part of the work on Pu will be the measurement of phonon dispersion curves from single crystals. This work will require a significant effort to develop experimental techniques and software for the analysis of phonon dispersion curves with a time-of-flight instrument. Software for this work will be developed in the software effort proposed for the HELIOS spectrometer. A larger user program and a higher level of

scientific activity associated with the presence of HELIOS will help the development of experimental methods needed for single crystal work with PHAROS.

Some experimental problems will benefit from the use of both PHAROS and HELIOS. Measurements of phonon dispersion curves from small single crystals of ^{242}Pu are expected to be limited by neutron flux. The most appropriate way to perform these experiments is to start by making several precise measurements on PHAROS. The excellent energy resolution of the PHAROS spectrometer will facilitate the identification of the phonon dispersion curves. For measurements at many different crystal orientations or at different pressures and temperatures, however, it would be most appropriate to use an instrument such as HELIOS, which offers much stronger signals. The flexibility of having the HELIOS instrument to complement PHAROS will facilitate all inelastic scattering research at LANSCE, including the weapons efforts.

1.4 User Program

Because the energy resolution of HELIOS will be similar to that currently attainable on thermal beam triple axis spectrometers, to some extent, the user base will mirror that of that class of instruments. However, HELIOS will offer dramatically improved efficiency for measurements of dynamics over wide ranges of frequency and momentum space. Firstly, HELIOS will offer dramatically improved sensitivity to inelastic scattering with energy transfer between 50 meV and 500 meV. Secondly, the large solid angle detector bank will enable experiments on systems where the scattering is distributed over a wide range of energies and momenta, as is the case for many novel magnetic systems that do not possess well-defined dispersion surfaces. Even for more traditional mapping of dispersion surfaces the phase space gains can be substantial since large regions of (\mathbf{Q}, ω) must be surveyed in order to locate all propagating modes.

2 Instrument Description

HELIOS will be installed on Flight Path 8 in ER-1 viewing the high intensity water moderator. The layout of the instrument is shown in [Figure 5](#). The philosophy guiding the design of the instrument is the desire to maximize the flux at the sample position and the solid angle detector coverage. This must be achieved with an energy resolution appropriate for the scientific program described in Section 1 (typically 2-5% of E_i , similar to that commonly employed on triple axis spectrometers). The instrument is designed for single crystal measurements from the outset. This implies a goniometer for crystal rotation and a detector array consisting of linear position sensitive detectors where gaps in coverage are minimized. The short 2.5 m secondary flight path allows us to span scattering angles between -20 and 140° in the horizontal plane and $\pm 10^\circ$ in the vertical plane with a relatively inexpensive 5.5 m^2 detector bank. We will use the LRMECS spectrometer at Argonne for component testing as needed. A detailed description of the essential features of the design follows in Sections 3.1-3.4.

Wherever possible we have tried to adopt hardware that is similar to that employed on PHAROS. This simplifies things from both the user and facility perspective. There are a number of interface issues that must be coordinated with LANSCE:

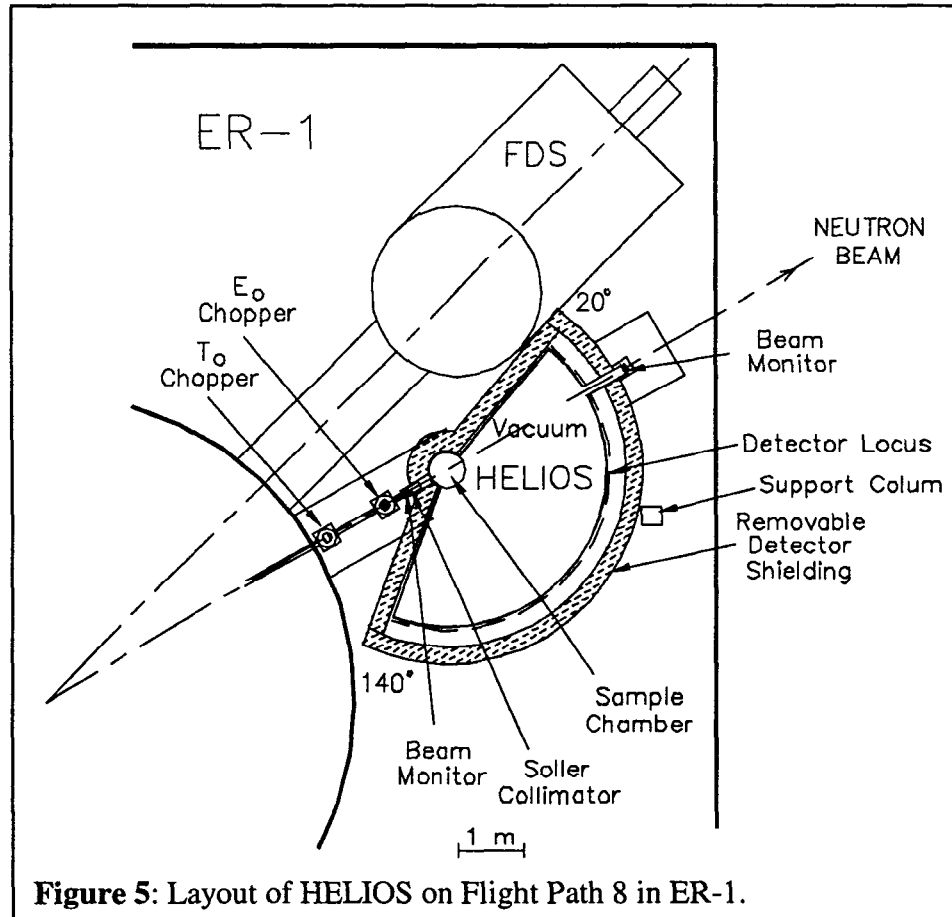


Figure 5: Layout of HELIOS on Flight Path 8 in ER-1.

- The spectrometer is being installed in a very restricted space in ER-1. This does not pose a major problem due to the desire for a compact instrument to maximize neutron intensity. However, there is a load bearing post very close to FP-8 (shown in [Figure 5](#)) which will make accessing the detectors for installation and servicing difficult if the design is not carefully thought out.
- The phasing of the chopper to the source will require a TTL pulse, likely HELIOS will operate slaved to PHAROS which has much more stringent timing specifications due to its higher resolution.
- The catwalk providing access to the back of ER-1 runs over top of FP-8. Support currently in place may have to be reconfigured. There is not a large load associated with this so it can likely be incorporated into the bulk shielding and vacuum vessel.
- The sample environment inserts will be subject to the same safety concerns as other cryogenic and furnace systems in use at the Lujan Center.
- The vacuum vessel, while not as large as that being installed on PHAROS, still requires careful engineering to insure it can be operated safely.

2.1 Incident Flight Path

HELIOS will be located on flight path 8 in ER-1 viewing the “high-intensity” H₂O moderator. For much of the energy range, this provides a twofold increase in intensity over the “high-resolution” H₂O moderator viewed by PHAROS, and the pulse widths,

which vary from 4 μ s at 1eV to 25 μ s at 10 meV, are better matched to the reduced primary and secondary flight paths. We estimate that the incident flux will be at least factor three greater than available on HET for the equivalent elastic resolution of 5% of the incident energy (FWHM) (see Section 3.4).

The main components of the beam-line outside the biological shielding are:

- 1) The background-suppressing T-zero chopper
- 2) The monochromating Fermi chopper
- 3) Adjustable slits
- 4) Supermirror guide

One of the important advantages of direct-geometry chopper spectrometers on pulsed neutron sources is the flexibility that they provide the experimenter in optimizing the incident energy and resolution of the measurements. The incident energy can be varied from 10 meV to 1 eV by changing the Fermi chopper phase, speed, and, occasionally, the slit package. HELIOS will take full advantage of this flexibility with three Fermi chopper slit packages to allow the measurement of energy transfers from 1meV to 500 meV.

2.1.1 Biological Shielding

The visible area of the “high-intensity” H₂O moderator viewed by HELIOS is 12.5 x 12.5 cm². The primary collimation within the biological shielding consists of B₄C apertures of tapering size. One of the options that we wish to consider in more detail is the ability to switch between this standard collimation and a supermirror guide, also installed in the biological shielding. This would have substantial intensity benefits at the lower end of the HELIOS energy spectrum, below 40 meV, particularly if coupled to focusing guides before the sample position. Such guides have been successfully installed close to the cold sources of reactors without suffering significant radiation damage. However, it may not be compatible with the current mercury shutter mechanism used most commonly at MLNSC. We will perform more detailed Monte Carlo estimates of the flux gains before proceeding with this option.

2.1.2 T₀ Chopper

The purpose of the T-zero (T₀) chopper, which will be located just outside the biological shielding at about 5.1 m from the moderator, is to suppress both the prompt pulse of fast neutrons produced when the proton-beam strikes the target and the time-independent background arising from delayed neutrons from the moderator. The HET spectrometer at ISIS has a nimonic alloy chopper with two fins that block the beam only during the prompt pulse. Since this has no effect on the delayed neutrons, the backgrounds were considerably higher when the uranium target was in operation. Moreover, the downstream Fermi chopper modulated the delayed neutron background making it extremely difficult to subtract reliably.

We therefore propose to use a coarse Fermi chopper which can be phased to the incident energy of the monochromating Fermi chopper while running at a lower multiple of the source pulse frequency. Beryllium-bodied choppers running on mechanical bearings have proved to be very effective on the HRMECS and LRMECS spectrometers at IPNS. They

are identical in design to the Fermi choppers but have no collimating slit packages so the transmission for in-phase neutrons is 100%. The kinematics of the neutron scattering processes ensure that the chopper is closed up to very high fractional energy transfers so that backgrounds are reduced over the useful portion of the time frame. Care has to be taken that detector backgrounds are not increased during subsequent open periods of the chopper.

2.1.3 Fermi Chopper

The Fermi chopper will be located at 6.1 m from the moderator. Its purpose is to produce a monochromatic burst of neutrons whose energy is determined by the chopper phase. The intensity and resolution of the neutron pulse incident on the sample is governed by both the chopper rotation frequency, which can be any integer multiple of the source frequency up to a maximum of 600 Hz, and the dimensions of the curved collimation slits within the chopper. The relevant dimensions are the slit width, the slat width, radius of curvature and external radius of the chopper body. Although precise optimization of the intensity and resolution requires the ability to vary all these parameters, a set of three chopper slit packages provide adequate performance over the entire range of accessible energy transfers, from 1 to 500 meV.

We present in [Figure 7](#) (Section 3.4) estimates of the intensity and resolution of three different chopper slit packages. They are labeled by the energy of their maximum transmission at a rotation frequency of 600 Hz. The following parameters were used:

	Slit Width	Slit Width	Curvature	Body size
250 meV	1.29 mm	0.55 mm	920 mm	49 mm
100 meV	2.58 mm	0.55 mm	580 mm	49 mm
12 meV	5.77 mm	0.55 mm	200 mm	49 mm

In order to achieve rotation speeds up to 600 Hz, the Fermi chopper will employ magnetic bearings. These have the added advantage of better phase stability than mechanical-bearing choppers.

A critical development priority for the HELIOS project is to determine how the Fermi chopper system will be timed to the source pulse. At present, the MLNSC has only one chopper spectrometer, PHAROS. The phase of its Fermi chopper tracks frequency variations in the external power supply and triggers the proton beam injection accordingly. There are proposals to change the timing electronics of the PHAROS chopper system, so HELIOS will be designed in conjunction with those changes. There is also considerable investment in chopper electronic and computer control developments by SNS and IPNS. The chopper phasing mechanisms will be tested during the development phase on the LRMECS spectrometer before final construction at Los Alamos.

2.1.4 Adjustable Slits

We will install two sets of adjustable slits in order to reduce backgrounds when samples smaller than the overall beam size are being measured. They will be installed both in the Fermi chopper housing and just before the sample chamber with both horizontal and vertical adjustment. Since both locations will be inaccessible when safety interlocks are in place, the slits will be fitted with stepper-motor drives for remote operation.

2.1.5 Supermirror guide

The angle subtended by a detector pixel is 0.6° (see Section 3.3) corresponding to a FWHM angular divergence of 0.3° for a point sample. The distance collimation associated with a point sample viewing a $12.5 \times 12.5 \text{ cm}^2$ moderator at 7.1 m is 0.5° giving a reasonably well matched initial and final divergence, particularly once the effect of finite sample size (which impacts final divergence to a greater extent due to shorter distance) are taken into account. Nevertheless, there are many cases where the increased intensity that can be achieved at the expense of beam divergence by using supermirror guide in the incident flight path. In principle the guide should extend as far back to the source as possible, into the biological shield described in 3.1.1. However this may be ruled out by compatibility with the mercury shutter. In the event this is the case we would still include a shorter guide section in the section between the two choppers. This would be installed on a cylindrical drum that is aligned parallel to the beam thus permitting a variety of beam conditioning optical elements to be remotely inserted as dictated by the needs of the experiment. The detailed choices for insertion would be based on the results of the Monte Carlo optimization but the flexibility offered by straight and tapered guide sections, along with smaller aperture channels for smaller samples with reduced background would greatly increase the flexibility of HELIOS. The cost estimate in Section 4 is based on the assumption a full guide section can be installed. If we are restricted to a shorter section then the savings in guide costs can be devoted to the rotating insertion device.

2.2 Vacuum Vessel

The vacuum vessel of HELIOS serves three purposes. It provides an evacuated secondary flight path, a low background environment for the detector bank, and vacuum insulation for certain sample environments. The inner volume of the vessel will be a 160 degree wedge of a cylinder with a radius of approximately 2.6 m and height 1.1 m. With these dimensions the inner volume of the vessel will be 10 m^3 while the surface area is 33 m^2 . The vacuum vessel will be built from approximately 0.75" thick steel plates with a total mass of $4 \times 10^3 \text{ kg}$. The mass of support structures is estimated to be $2 \times 10^3 \text{ kg}$ so that the total mass of the vacuum vessel will be about 6 metric tons. This exceeds the capacity of the crane in ER-1 so we plan to use rollers in combination with a fork truck to bring the vessel to its location there. At present we anticipate that the detectors will be mounted in vacuum within the vessel since we estimate that it is easier to create a vacuum feed-through for the detector cables than establish thin windows which sustain an atmosphere. No extra expenditure will be made for non-magnetic steel since a magnetically polarizable vacuum vessel should not preclude future production or detection of polarized

neutrons. In addition much of the science to be pursued does not require polarization analysis.

Because of the high ability of the internal neutron shielding (crispy mix) to adsorb water it is probably not practical to pump the whole vacuum vessel down to the cryogenic vacuum required for sample environments. The vessel will therefore have a sample vacuum separated from the main vacuum by a very thin aluminum or sapphire membrane at beam height (<0.1 mm). This differential shield will only have to support a pressure difference of approximately 0.1 mbar corresponding to a force of 10^{-2} N/m² and it will be stationary with respect to the incident beam. The main cost for this item, estimated at \$10,000, will go to developing the evacuation and safety interlock system to prevent there from being a pressure difference larger than 0.1 mbar between the sample and detector volumes.

2.2.1 Shielding requirements

For maximum dynamic range in inelastic scattering experiments it will be crucial to provide a low background environment for the HELIOS detector bank. For this reason the vacuum vessel will be surrounded by a 20-30 cm thick shell of shielding. Thin walled steel containers will be filled with a mixture of wax and borax (Na₂B₄O₇), for moderation and absorption of neutrons which would otherwise enter the detector bank from the outside. To determine the thickness and composition of the shielding required experiments will be conducted at Flight Path 8 with a single PSD detector in a small shielded volume of varying composition and wall thickness. In anticipation of future proton current upgrades and taking into account previous unpleasant experiences in which shielding requirements were underestimated we will tend to be generous with shielding material. With a mass ratio of 25% borax powder and 75% wax the density of the shielding material will be approximately 1 g/cm³. There will be shielding on all sides of the vacuum vessel and the corresponding shielding volume will be 6-9 m³ with a mass of 6-9 metric tons. Naturally this shielding will be segmented so that it can be brought into place using the crane in ER-1. At an estimated price of 1000\$/m² the total cost of shielding the vacuum vessel will be \$33,000 including design costs. Special attention must of course be paid to shielding around the incident beam path and to completely coating the inside of the vessel with boron loaded epoxy (crispy mix). The price for crispy mix is \$2000/m² so we will use \$66,000 for this purpose.

2.2.2 Vacuum pumping system

The pumping system will be designed with the following constraints.

1. It must be completely automated and equipped with interlocks for safety and to protect the investment
2. It must be able to bring the entire vacuum vessel from ambient pressure to base pressure in 1 hour.

3. It must achieve a base pressure of 10^{-3} mbar in the main vessel and 10^{-6} mbar in the sample vacuum chamber.
4. It must avoid cryopumping of water and other material onto a sample held at 3.6 K.
5. It should not require service or regeneration under normal operating conditions over the period of a typical LANSCE beam cycle

For rapid pump down of the entire vessel to 10^{-3} mbar we shall use a root pump backed by a conventional rotary pump. The required pumping speed is of order 1000 cubic feet per minute. A suitable system costs approximately \$ 60,000. To reach a pressure of 10^{-6} mbar in the sample vacuum we shall use a turbo molecular pump at a price of \$15,000. To avoid cryopumping onto the sample the sample volume will also be pumped by a cryo-pump (poly-cold) estimated to cost \$30,000. Finally to maintain a dry atmosphere in the vessel at all times we shall purchase a dry air venting system estimated at \$15,000. From the experience building PHAROS we estimate that design and construction of the pumping automation and interlock system will cost \$15,000.

2.3 Detectors

The detector array on HELIOS will consist of 262 linear position sensitive detectors (LPSDs) of the same type used on PHAROS. These are 2.5 cm x 90 cm tubes which will be electronically resolved as 36 2.5 cm x 2.5 cm pixels, for a total of 9432 individual detector elements. Each pixel will subtend 0.6° , corresponding to a FWHM angular resolution of 0.3° , comparable to the mosaic spread of typical single crystals. For powder samples the detector array will be decomposed into Debye-Scherrer rings. Angles from -20° to $+140^\circ$ in the horizontal plane and ± 10 degrees vertically will be accessed with even spacing of the detectors to the extent possible while maintaining the structural integrity of the vacuum vessel. The detector array and associated electronics are the single most expensive component of HELIOS. However, the wide angle coverage translates directly into improved detection efficiency and the combination of low angles for magnetic studies and high angles for phonon measurements is essential to the two components of the scientific program.

2.4 Computer systems

The data acquisition and analysis systems will be built using commodity components following the standard under development at LANSCE and IPNS. Software for HELIOS will benefit from (and provide benefits to) similar systems employed on PHAROS and ISIS. The software required to visualize and carry out lineshape analysis of data obtained on HELIOS will be developed at Oak Ridge in a generic form making it suitable for single crystal time of flight data obtained at any facility. By adhering to the emerging, HDF based, NeXus data format portability of HELIOS data to this (or any other analysis package) will be ensured.

2.4.1 Data acquisition

The data acquisition hardware will be a modular VME based system which will provide the necessary event timing and positioning. An ethernet connection to the host UNIX or Windows NT computer will be sufficient for the data rates anticipated on HELIOS (the

full detector images are large but for typical inelastic experiments counting times are long so a delay of a few seconds is tolerable). The user interface to the data acquisition will be via a web browser, decoupling the location and operating system of the spectrometer from those of the user. The sample environment will also be controlled via a web browser interface through the use of Labview and IEEE-488 or RS-232 interfaces. Password based security, which is specific to a given experiment, will ensure safe and secure remote operation. Only systems that can be modified without compromising safe operation will be remotely controllable although all relevant machine parameters will be viewable.

2.4.2 Experiment simulator

An online experiment simulator will be built up from the Monte Carlo code used to optimize HELIOS. In order to be useful for real time experiment optimization it will be restricted to resolution modeling (i.e. the full instrument performance including background will not be simulated). This will be accessed from the same software interface as the analysis package or as a callable routine from user supplied software.

2.4.3 Data analysis and presentation

One of the computational challenges facing large solid angle chopper instruments is dealing with the visualization of thousands (9432 for HELIOS) of time of flight scans each constituting a trajectory through the four dimensional (\mathbf{Q},ω) space of a single crystal sample. Each time of flight trajectory itself consists of thousands of microsecond time bins. The software must correctly transform the data from (ϕ,t) [angle and time] into (\mathbf{Q},ω) keeping track of resolution volume, statistical uncertainty, detector efficiency, and crystal coordinate transforms. Having done this the data must then be projected onto a two dimensional space appropriate for the scientist to view and make decisions about the next step in the experiment. The data from a single setting of the spectrometer will be projected, sliced, viewed, and modeled in attempt to reconstruct the important features of the dynamical response of the sample being measured.

Fortunately, powerful tools exist for manipulating and visualizing large arrays of data. Commercial programs such as IDL and Matlab greatly reduce the development time for specialized software to handle this problem. However, HELIOS and PHAROS II will have more than an order of magnitude more detector elements than any existing time of flight spectrometer (due to the use of spacially resolving LPSDs) so they will tax the hardware and software capabilities of whatever system is adopted.

2.5 Sample environment

Sample environments will be provided by units that mount on a rotating stage atop the HELIOS vacuum vessel. The stage will have a rotating vacuum seal large enough to enclose the LANSCE standard bolt circle. The different systems for sample environment to be mounted with this bolt circle are:

1. Thimble, a thin-walled aluminum containment to separate the spectrometer vacuum from a cylindrical specimen region at ambient pressure. Specialized sample environments provided by users will fit within this thimble.
2. Low temperature heliPLEX system for experimentation from 3.6 K to 350 K. This unit is a closed-cycle refrigerator with enhanced low temperature capability provided by a Joule-Thompson heat exchanger.
3. Displex/heater unit for a temperature range of <30 - 650 K.
4. High temperature furnace unit capable of temperatures from 600 - 2073 K.

These units are described in detail below. An over-riding consideration in choosing these units was their ease-of-use. Especially in the early years of HELIOS, all users will be inexperienced with its characteristics. Further risk to the users' experiments caused by complexities of cryostat control, for example, are important to avoid. Displex units also provide for more convenient computer interfacing, and promise a greater degree of automatic control of data acquisition.

2.5.1 Sample rotation stage

Much of the science to be done on HELIOS involves single crystal samples. For these experiments it is necessary to orient the reciprocal space of the sample with respect to the wave vector transfer probed by the spectrometer. For a given choice of E_i a conventional triple axis spectrometer can probe the neutron scattering cross section for wave-vector transfer on part of a circle of radius k_f which is displaced from the origin by \mathbf{k}_i . For a given value of $Q=|\mathbf{k}_i-\mathbf{k}_f|$ there are at most two orientations of the sample which will bring a given reciprocal lattice direction into coincidence with $\mathbf{k}_i-\mathbf{k}_f$. To probe an arbitrary value of wave *vector* transfer to the sample it is therefore necessary on such an instrument to select the tilt of the sample about an arbitrary horizontal axis as well as to rotate the sample about a vertical axis. On HELIOS the tall Position Sensitive Detectors (PSD) subtend a vertical angular range of 20 degrees such that for a given choice of E_i the detector bank probes an equatorial band on the surface of a sphere of radius k_f which is displaced by \mathbf{k}_i from the origin of reciprocal space. The detector bank thus probes an area in reciprocal space and there are lines along this spherical band which correspond to specific values of $Q=|\mathbf{k}_i-\mathbf{k}_f|$. This implies that for a given choice of E_i and E_f a volume of reciprocal space can be accessed on the HELIOS detector bank with just a vertical axis of rotation for the sample. If only values of wave vector transfer within a specific reciprocal lattice plane are of interest, it will be necessary to orient this plane of the crystal lattice to within 5 degrees of the horizontal plane. This level of accuracy is easily obtained using well-established alignment techniques. It is therefore sufficient on HELIOS to implement a rotation stage capable of rotating the sample about a vertical axis.

The rotation stage will include the flange for mounting the sample environment units atop the vacuum vessel. This requires the design of a rotating vacuum feed through. The diameter of the LANSCE standard bolt circle (as on PHAROS) will set the size of the sample environment units. In cases where further degrees of freedom for sample orientation with respect to the spectrometer are required this will have to be accomplished through specialized goniometers within the sample environment. The sample rotation

stage will be based on a commercial rotation table. A stepping motor and associated controller connected to the data acquisition software through an IEEE interface will control the angular setting of the rotation stage to within an accuracy of 0.01 degrees.

2.5.2 Thimble for specialized sample environments

While most sample environments will use the vacuum of the HELIOS vacuum vessel to provide an evacuated scattering volume and thermal insulation is necessary there are cases in which special conditions require a separate sample vacuum. Examples of such cases are

1. When the HELIOS vacuum vessel does not provide adequate thermal insulation as for example in the case of a dilution refrigerator.
2. When there is a risk that the sample may disintegrate and contaminate the main vacuum vessel as in the case of the high temperature furnace.
3. When it is necessary to have access to a sample vacuum prior to availability of the HELIOS vacuum vessel.
4. When a specialized sample environment, which cannot be mounted directly on the rotating vacuum flange, is to be used.

For these and other cases there will be an ambient pressure thimble that can be mounted on the rotating vacuum flange to provide ambient pressure and temperature access to the HELIOS scattering volume. The thimble will be made of aluminum tube stock and have a thin aluminum window at beam height to minimize scattering from this part of the sample environment. The thickness of this window will be in the range 1-2 mm as dictated by strength and safety considerations. All parts of the thimble outside of beam height will be coated with neutron absorbing material such as boron loaded epoxy on the side facing the vacuum vessel.

2.5.3 Oscillating radial collimator

Important parts of the scientific projects to be pursued on HELIOS involve sample environments that necessarily place significant amounts of material in the incident beam path. Examples are the high temperature furnace and various high pressure cells to be used on the instrument. Owing to their different flight paths, neutrons which scatter elastically from material that is not at the sample position will in general arrive at the detector bank at different times than neutrons which scatter elastically from the sample. The result can be intense spurious that are difficult to distinguish from inelastic scattering from the sample itself.

To suppress these spurious and background, HELIOS will be equipped with an oscillating radial collimator. The collimator will be located in the detector vacuum vessel in such a way that it can be used in combination with any sample environment including the ambient pressure thimble. The collimator will cover the full angular range of the detector bank and the blade spacing will be chosen so as to define a cylindrical scattering volume with a diameter of order 1 cm. With an inner diameter of approximately 0.5 m this

requires a collimation of approximately 140 minutes of arc per channel. Assuming a blade length of 30 cm, the entire collimator would have of order 60 blades separated by approximately 1.2 cm. There are several companies that have delivered such collimators in the past. We are basing our price estimate on the cost for the radial collimator purchased by John Copley of NIST from Euro Collimator in 1997. One innovation would be the necessity of using a neutron absorbing material such as boron, which remains efficient up to neutron energies of order 500 meV. Given the large blade spacing we believe this problem can be solved without reducing the transmission of the device below 90 %.

The radial collimator will be mounted on a rotation stage to provide the oscillating motion that prevents permanent shading of specific directions. Not only the collimator blades but also the frame from which the blades are suspended and the rotation stage will be coated with neutron absorbing material to avoid spurious scattering processes. Provisions will be made to automatically lower or raise the collimator out of the beam path when it is unnecessary.

2.5.4 Low temperature closed-cycle refrigerator (3.6 - 350 K)

A closed-cycle refrigerator unit is already in place at LANSCE for use on PHAROS, and we expect this unit to be adaptable to HELIOS. Since low temperatures are required for much of the scientific program, it is important to acquire another displer unit. We may choose to duplicate the PHAROS unit, but our preference is to obtain a unit with extended low temperature capability. One approach is taken by APD Cryogenics in their commercial Heliplex design. It uses a closed-cycle refrigerator in combination with a Joule-Thompson heat exchanger to achieve base temperatures below 3.6 K. A temperature controller dedicated to this device will be purchased.

2.5.5 High temperature closed-cycle refrigerator (<30 - 650 K)

Ross W. Erwin of NIST has modified a closed-cycle refrigerator to enable it to reach temperatures of 650 K. The trick is to use a sapphire spacer between the cooling head and heating stage. The thermal conductivity of sapphire is temperature-dependent so that it provides better heat conduction at low temperatures than at higher temperatures. The NIST group is agreeable to providing us with drawings and technical advice. We plan to build our own unit, however, which is based on a closed-cycle refrigerator unit from APD or Leybold, a heating stage from Air Products, and a sapphire link between them. Although the closed-cycle refrigerator has a base temperature of 6.5 K, we expect that with the sapphire spacer the base temperature should be between 25 and 30 K. A temperature controller dedicated to this refrigerator will be purchased.

2.5.6 Furnace (600 - 2073 K)

We have evaluated the performance and reliability of several high temperature furnaces that have been used previously for neutron scattering work. The clear choice is the "ILL" furnace manufactured by AS Scientific Products, Abingdon, England, and shown below

in [Figure 6](#). This unit uses a cylindrical Nb heating element around the sample, which can be as large as 4.5 cm diameter and 10 cm high. Cylindrical Nb radiation shields surround the heating element, and the water-cooled housing has thin Al windows for 360° neutron access around the sample. Neutron access is $\pm 20^\circ$ out of the plane of the spectrometer. This unit has relatively low background, but the background will be essentially negligible with incident beam collimation and the use of radial collimators in the HELIOS vacuum vessel. The unit is reasonably priced, about 65 k\$ with vacuum system, power supply, interlocks, and miscellaneous spare parts.

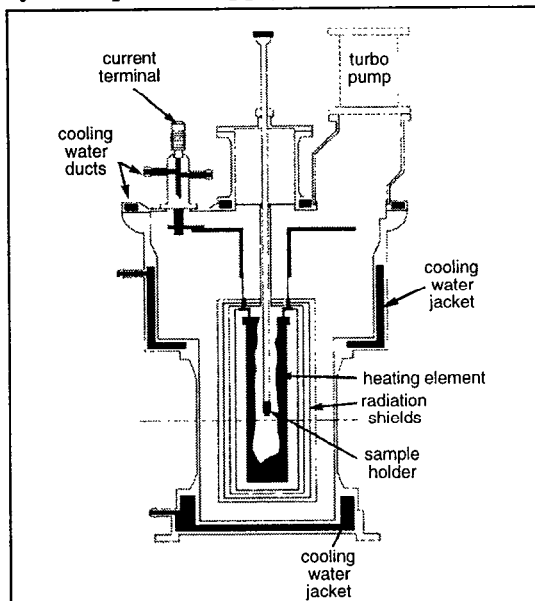


Figure 6: The ILL high temperature furnace. The thin Nb heating element and Nb radiation shields are in the neutron beam, but we have had little trouble with spurious scattering in reactor experiments with collimated beams at ORNL.

An important advantage of this ILL furnace is that it is a mature product, with an integrated vacuum system, temperature controller, power supply, and safety interlocks. It will likely be useful for other experimental facilities at LANSCE — certainly it will be useful on PHAROS. There is a possibility that an ILL high temperature furnaces will be procured for the PHAROS spectrometer. Depending on timetable and funding for HELIOS, it may be possible to find partial external support for this furnace as it is being purchased for work on PHAROS.

2.5.7 Issues with pressure cells

Pressure experiments with a samples having masses of tens of grams and greater are often performed by mounting the sample in a canister that can be compressed in a hydraulic press, and then locked in a compressed position. Upon removal from the hydraulic press, the pressure is maintained in this “pressure cell”, which is a compact unit that can be moved into the specimen region of the HELIOS spectrometer, for example. An obvious feature of the pressure cell is that it is made of high strength materials such as sapphire or steel, and typically more such material when higher pressures are required. For pressures of 10 kbar or higher, spurious scattering from the pressure cell can overwhelm the scattering from the sample itself. This problem can be alleviated considerably by collimation. The incident beam is collimated to have a width comparable to the sample, and the scattered beam is collimated with the oscillating radial collimators. The small size of the vacuum vessel of HELIOS facilitates such scattered beam collimation with oscillating radial collimators. For this reason we expect it to be easier to perform high pressure experiments with HELIOS than with the PHAROS spectrometer.

2.6 Projected system performance

To complement PHAROS II, which was optimized for high resolution, HELIOS will be optimized for high flux and sensitivity with a correspondingly coarser energy resolution. As a rough measure of the overall sensitivity of the two instruments we take:

$$\eta = \Omega_i \Delta E_i / E_i \Omega_f, \quad (4)$$

where Ω_i is the solid angle by which the moderator is viewed from the sample position, Ω_f is the total solid angle of the detection system, and $\Delta E_i / E_i$ is the relative energy resolution of the Fermi chopper system. The estimated values for these quantities are:

Instrument	Ω_i (steradians)	$\Delta E_i / E_i$	Ω_f (steradians)
PHAROS II	3.9×10^{-5}	0.5%	0.65
HELIOS	3.1×10^{-4}	5%	1.1

For HELIOS we have not taken into account the enhancement in solid angle Ω_i by as much as a factor of 2 for $E_i < 30$ meV which will be achieved through the use of a super mirror guide in the incident beam path. Nor have we considered the higher flux at the coupled HELIOS moderator as compared to the decoupled water moderator at PHAROS. From these numbers we obtain a lower bound on the ratio of sensitivity between the two instruments:

$$\eta_{\text{HELIOS}} / \eta_{\text{PHAROS}} > 2 \times 10^2 \quad (5)$$

This estimate is perhaps the best argument for building HELIOS. For scientific projects such as those described in Section 2 which do not require very good energy resolution, it will be possible to complete experiments on HELIOS in days, which could not be completed on PHAROS in an entire cycle. On the other hand HELIOS does *not* supersede PHAROS because it will not be useful for experiments which do require $\Delta E_i / E_i < 3\%$. Nor will it provide access to the very low angle regime which is important for probing sound waves in amorphous solids and liquids. The two spectrometers are therefore manifestly complementary. With both, LANSCE will have a productive suite of spectrometers around which to develop a world class scientific program in the important fields of condensed matter physics and materials science outlined in this proposal. With only PHAROS, LANSCE will *not* be competitive for probing dynamics of solids in the important thermal and epithermal energy ranges.

For an absolute comparison of HELIOS to similar instrumentation at other spallation sources, T. G. Perring calculated flux and resolution as a function of incident neutron energy using software that he has developed and verified for accuracy at ISIS. Again we seek a conservative estimate so the calculation does not taken into account the supermirror guide or the coupled moderator which will enhance the flux without

compromising resolution. The parameters which went into the calculation are listed in [Table 1](#). The result of the calculations are shown in [Figure 7](#).

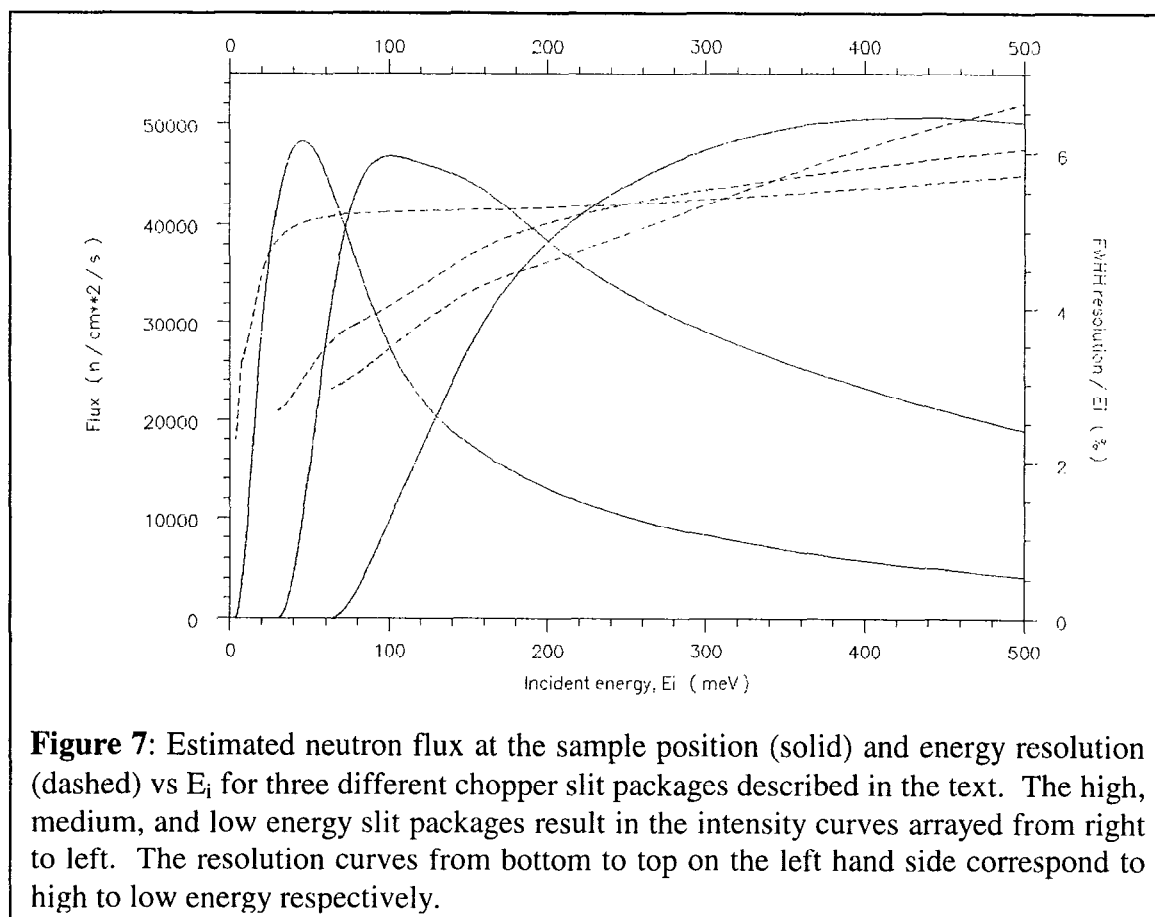


Figure 7: Estimated neutron flux at the sample position (solid) and energy resolution (dashed) vs E_i for three different chopper slit packages described in the text. The high, medium, and low energy slit packages result in the intensity curves arrayed from right to left. The resolution curves from bottom to top on the left hand side correspond to high to low energy respectively.

There are three pairs of curves showing flux and resolution for three different Fermi chopper slit packs optimized for $E_i=20$ meV, $E_i= 100$ meV, and $E_i= 400$ meV and $\Delta E_i/E_i=5\%$. One important observation is that the peak flux and relative energy resolution for these chopper systems is almost energy independent from 20-500 meV. It is also clear from these calculations that this impressive energy range can only be accessed with several different Fermi chopper slit packs. The HELIOS chopper system will be designed to minimize turn around time for changing the incident energy and the Fermi chopper. The energy resolution plotted is the elastic linewidth, the energy resolution decreases as the energy transfer is increased so most excitations will be measured with tighter resolution than that implied by [Figure 7](#).

Moderator to Chopper Distance	6.1 m
Chopper to sample distance	1 m
Sample to detector distance	2.5 m
Moderator area	12.5 cm x 12.5 cm
Moderator type	Water T=316 K poisoned at 1.5 cm

Target	ISIS Tantalum target
Proton beam power	160 kW

Table 1. Specifications underlying the flux and resolution calculations of [Figure 7](#).

The other important message from [Figure 7](#) is the absolute flux numbers. At $E_i=100$ meV the flux on HELIOS will exceed the maximum monochromatic flux which can currently be obtained on MARI by roughly a factor 3. Of course this is simply due to the larger incident bandwidth and beam divergence on HELIOS. This does mean, however, that HELIOS would bring a world record in pulsed monochromatic flux to LANSCE, and that it would attract experimenters with projects which require high sensitivity at a relative energy resolution similar to that of a triple axis spectrometer.

3 Conclusions

HELIOS combines the relatively coarse resolution, and therefore high single to noise, of a thermal triple axis spectrometer with the dynamic range and efficiency of a high solid angle direct geometry time of flight spectrometer. It will permit the application of neutron spectroscopy to a wide range of problems that currently cannot be addressed due to limitations associated with small sample size, weak scattering, or demanding sample environments.

Acknowledgements

We would like to thank T.G. Perring for assistance with comparisons of flux and resolution with ISIS instruments. Work at Oak Ridge was carried out under U.S. Department of Energy Contract No. DE-AC05-96OR22464. T.E.M. acknowledges the support of NSERC, CIAR, and the A.P. Sloan Foundation for work carried out at the University of Toronto.

References

- ¹ See, for example: F. Ducastelle, Order and Phase Stability in Alloys, (North Holland, Amsterdam, 1991).
- ² L. Anthony, J. K. Okamoto, and B. Fultz, "Vibrational Entropy of Ordered and Disordered Ni_3Al ", *Phys. Rev. Lett.* **70** (1993) 1128-1130.
- ³ L. Anthony, L. J. Nagel, J. K. Okamoto, and B. Fultz "The magnitude and origin of the difference in vibrational entropy between ordered and disordered Fe_3Al ", *Phys. Rev. Lett.* **73** (1994) 3034-3037.
- ⁴ L. J. Nagel, L. Anthony and B. Fultz, "Differences in vibrational entropy of disordered and ordered Cu_3Au ", *Philos. Mag. Lett.* **72** (1995) 421-427.

- ⁵ L. J. Nagel, B. Fultz, and J. L. Robertson, "Vibrational Entropies of Phases of Co_3V Measured by Inelastic Neutron Scattering and Cryogenic Calorimetry", *Philos. Mag. B*, in press.
- ⁶ B. Fultz, L. Anthony, L. J. Nagel, R. M. Nicklow and S. Spooner, "Phonon densities of states and vibrational entropies of ordered and disordered Ni_3Al ", *Phys. Rev. B* 52 (1995) 3315-3321.
- ⁷ L. J. Nagel, B. Fultz, J. L. Robertson, and S. Spooner, "Vibrational entropy and microstructural effects on the thermodynamics of partially-disordered and ordered Ni_3V ", *Phys. Rev. B*, 55 (1997) 2903-2911.
- ⁸ B. Fultz, J. L. Robertson, T. A. Stephens, L. J. Nagel and S. Spooner, "Phonon density of states of nanocrystalline Fe prepared by high energy ball milling", *J. Appl. Phys.* 79 (1996) 8318-8322.
- ⁹ H. N. Frase, L. J. Nagel, J. L. Robertson, and B. Fultz, "Vibrational Density of States in Nanocrystalline Ni_3Fe ", *Philos. Mag. B* 75 (1997) 335.
- ¹⁰ T.G. Perring, G. Aeppli, S.M. Hayden, S.A. Carter, J.P. Remeika, and S.-W. Cheong, "Spin waves throughout the Brillouin zone of a double-exchange ferromagnet", *Phys. Rev. Lett.* 77 (1996) 711-714.
- ¹¹ T.E. Mason, C.P. Adams, S.A.M. Mentink, E. Fawcett, A.Z. Menshikov, C.D. Frost, J.B. Forsyth, T.G. Perring, and T.M. Holden, *Physica B* 237-238 (1997) 449-452.
- ¹² K. Yamada *et al.*, "An overall energy spectrum of magnetic fluctuations in the superconducting $\text{La}_{1.85}\text{Sr}_{0.15}\text{CuO}_4$ ", *J. Phys. Soc. Jpn.* 64 (1995) 2742.
- ¹³ S.M. Hayden, G. Aeppli, H.A. Mook, T.G. Perring, T.E. Mason, S.-W. Cheong, and Z. Fisk, "Comparison of the high-frequency magnetic fluctuations in insulating and superconducting $\text{La}_{2-x}\text{Sr}_x\text{CuO}_4$ ", *Phys. Rev. Lett.* 76 (1996) 1344.
- ¹⁴ P. Bourges, H.F. Fong, L.P. Regnault, J. Bossy, C. Vettier, D.L. Milius, I.A. Aksay, and B. Keimer, "High Energy Spin Excitations in $\text{YBa}_2\text{Cu}_3\text{O}_{6.5}$ ", *Phys. Rev. B* 56 (1997) R11439.
- ¹⁵ L. Soderholm, C.-K. Loong, and S. Kern, *Phys. Rev. B* 45 (1992) 10062.
- ¹⁶ R. Osborn, S. W. Lovesey, A. D. Taylor, and E. Balcar, "Intermultiplet transitions using neutron spectroscopy" in *Handbook on the Physics and Chemistry of Rare Earths*, edited by K. A. Gschneidner, Jr. and L. Eyring (North-Holland, Amsterdam, 1991), Vol. 14, p. 1.
- ¹⁷ A.T. Boothroyd, A. Mukherjee, A.P. Murani, "Evidence for extreme gap anisotropy in $\text{Ho}_{0.1}\text{Y}_{0.9}\text{Ba}_2\text{Cu}_3\text{O}_7$ from neutron spectroscopy of Ho^{3+} ", *Phys. Rev. Lett.* 77 (1996) 1600.
- ¹⁸ D.A. Tennant, R.A. Cowley, S.E. Nagler, *et al.*, "Measurement of the Spin-Excitation Continuum in One-Dimensional KCuF_3 using Neutron Scattering", *Phys. Rev. B* 52 (1995) 13368.
- ¹⁹ M. Arai, M. Fujita, M. Motokawa, *et al.*, "Quantum spin excitations in the spin-peierls system CuGeO_3 ", *Phys. Rev. Lett.* 77 (1996) 3649.
- ²⁰ A.W. Garrett, S.E. Nagler, *et al.*, "Magnetic excitations in the $S=1/2$ alternating chain compound $(\text{VO})_2\text{P}_2\text{O}_7$ ", *Phys. Rev. Lett.* 79 (1997) 745.
- ²¹ M. Ain, J.E. Lorenzo, L.P. Regnault, *et al.*, "Double gap and solitonic excitations in the spin-Peierls chain CuGeO_3 ", *Phys. Rev. Lett.* 78 (1997) 1560.

- ²² D.C. Dender , P.R. Hammar, D.H. Reich, C. Broholm *et al.* "Direct observation of field-induced incommensurate fluctuations in a one-dimensional S=1/2 antiferromagnet", *Phys. Rev. Lett.* 79 (1997) 1750.
- ²³ V. Kiryukhin, B. Keimer, J.P. Hill and A. Vigliante, "Soliton Lattice in Pure and Diluted CuGeO₃", *Phys. Rev. Lett.* 76 (1996) 4608.
- ²⁴ For a review, see E. Dagotto, T.M. Rice, "Surprises on the way from one- to two-dimensional quantum magnets: The ladder materials", *Science* 271 (1995) 618.
- ²⁵ M. Uehara , T. Nagata , J. Akimitsu, *et al.*, "Superconductivity in the ladder material Sr_{0.4}Ca_{13.6}Cu₂₄O_{41.84}", *J. Phys. Soc. Jpn.* 65 (1996) 2764.
- ²⁶ N. Motoyama, H. Eisaki , S. Uchida , "Magnetic susceptibility of ideal spin 1/2 Heisenberg antiferromagnetic chain systems, Sr₂CuO₃ and SrCuO₂", *Phys. Rev. Lett.* 76 (1996) 3212.
- ²⁷ See, for example, T. Katsufuji et al., "Spectral Weight Transfer of the Optical Conductivity in Doped Mott Insulators", *Phys. Rev. Lett.* 75 (1995) 3497, and references therein.
- ²⁸ Y. Maeno *et al.*, "Superconductivity in a layered perovskite without copper", *Nature* 372 (1994) 532.
- ²⁹ M. C. Aronson, R. Osborn, R. A. Robinson, J. W. Lynn, R. Chau, C. L. Seaman, and M. B. Maple, "Non-Fermi liquid scaling of the magnetic response in UCu_{5-x}Pd_x (x=1,1.5)" *Phys. Rev. Lett.* 75 (1995) 725.
- ³⁰ E. A. Goremychkin and R. Osborn, "Crystal field excitations in CeCu₂Si₂", *Phys. Rev. B* 47 (1993) 14280.
- ³¹ P. Soderlind, O. Eriksson, B. Johansson, J. M. Wills and A. M. Boring, *Nature* 374, 524 (1995), and references therein.
- ³² P. Soderlind, J. M. Wills, B. Johansson and O. Eriksson, *Phys. Rev. B* 55, 1997 (1997).
- ³³ J. L. Robertson, H. N. Frase, B. Fultz and R. J. McQueeney "Phonon densities of states of γ -Ce and δ -Ce measured by inelastic neutron scattering", submitted to *Phys Rev. Lett.*
- ³⁴ P. D. Bogdanoff, B. Fultz, J. L. Robertson, R. J. McQueeney, S. Rosenkranz, "Phonon Density of States and Heat Capacity of the Austenite-Martensite Transformation in the Shape Memory Alloy NiTi", manuscript in preparation.
- ³⁵ S. K. Satija, S. M. Shapiro, M. B. Salamon, and C. M. Wayman, "Phonon Softening in Ni_{46.8}Ti₅₀Fe_{3.2}", *Phys. Rev. B* 29 (1984) 6031. H. Chou and S. M. Shapiro, "Observation of predicted phonon anomalies in β -phase Ni₅₀Al₅₀", *Phys. Rev. B* 48 (1993) 16088.
- ³⁶ L. J. Nagel, B. Fultz, and J. L. Robertson, "Vibrational Entropies of Phases of Co₃V Measured by Inelastic Neutron Scattering and Cryogenic Calorimetry", *Philos. Mag. B* 75 (1997) 681-699.